JCI insight

RESEARCH ARTICLE

# DOCK8 is essential for LFA-1–dependent positioning of T follicular helper cells in germinal centers

**Erin Janssen,[1] Mira Tohme,[1] Jordan Butts,[1] Sophie Giguere,[2] Peter T. Sage,[3] Francisco E. Velázquez,[4] Christy Kam,[1] Elena Milin,[1] Mrinmoy Das,[1] Ali Sobh,[5] Salem Al-Tamemi,[6] Francis W. Luscinskas,[4] Facundo Batista,[2] and Raif S. Geha[1]**

[1]Division of Immunology, Boston Children's Hospital and Harvard Medical School, Boston, Massachusetts, USA. [2]Ragon Institute of Massachusetts General Hospital, Massachusetts Institute of Technology and Harvard Medical School, Cambridge, Massachusetts, USA. [3]Transplantation Research Center, Renal Division, Brigham and Women's Hospital and Harvard Medical School, Boston, Massachusetts, USA. [4]Center for Excellence in Vascular Biology, Brigham and Women's Hospital, Departments of Pathology and Medicine, Harvard Medical School, Boston, Massachusetts, USA. [5]Department of Pediatrics, Mansoura University Children's Hospital, Faculty of Medicine, Mansoura University, Mansoura, Egypt. [6]Sultan Qaboos University Hospital, Muscat, Oman.

**T follicular helper (Tfh) cell migration into germinal centers (GCs) is essential for the generation of GC B cells and antibody responses to T cell–dependent (TD) antigens. This process requires interactions between lymphocyte function–associated antigen 1 (LFA-1) on Tfh cells and ICAMs on B cells. The mechanisms underlying defective antibody responses to TD antigens in DOCK8 deficiency are incompletely understood. We show that mice selectively lacking DOCK8 in T cells had impaired IgG antibody responses to TD antigens, decreased GC size, and reduced numbers of GC B cells. However, they developed normal numbers of Tfh cells with intact capacity for driving B cell differentiation into a GC phenotype in vitro. Notably, migration of DOCK8-deficient T cells into GCs was defective. Following T cell receptor (TCR)/CD3 ligation, DOCK8-deficient T cells had impaired LFA-1 activation and reduced binding to ICAM-1. Our results therefore indicate that DOCK8 is important for LFA-1–dependent positioning of Tfh cells in GCs, and thereby the generation of GC B cells and IgG antibody responses to TD antigen.**

## Introduction

The antibody response to T cell–dependent (TD) antigens requires interactions between T follicular helper (Tfh) cells and B cells. Tfh cell differentiation is initiated upon T cell recognition of antigen presented by DCs in the interfollicular areas of lymph nodes (LNs) (1). Activated T cells migrate toward the B cell follicle, where they interact with B cells. This leads to the expression of Tfh cell–specific markers (2), including ICOS and programmed cell death 1 (PD-1) (3–5). The interaction of ICOS with ICOS-L on B cells induces expression of the transcription factor BCL6 (4, 5). In turn, BCL6 upregulates CXCR5 expression on Tfh cells (3, 4). CXCR5 drives the migration of Tfh cells toward CXCL13 produced by stromal cells in B cell follicles (6). Adhesion molecules, including lymphocyte function–associated antigen 1 (LFA-1), are important for T cell migration and retention in LNs (7, 8). Furthermore, the interaction between LFA-1 and ICAM-1/2 on B cells is critical for productive Tfh–B cell interactions leading to B cell clonal expansion (9).

In the germinal center (GC), Tfh and antigen-specific B cells that have acquired antigen from follicular DCs form strong, but short-lived contacts (10, 11). B cell signals are needed for the maintenance of the Tfh phenotype (12) and upregulate Tfh cell expression of IL-4 and IL-21 (11). Tfh cell production of IL-4 and IL-21, as well as the interaction between CD40L on Tfh cells and CD40 on B cells, are important for GC B cell proliferation, differentiation, BCL6 expression, and survival (13–15). GC B cells expressing a high-affinity B cell receptor for antigen compete more effectively for survival signals delivered by Tfh cells (16).

DOCK8 deficiency is a primary immune deficiency characterized by recurrent infections and diminished responses to vaccines (17–19). Similarly, the antibody response to TD antigens is impaired in *Dock8*$^{-/-}$ mice. While there are data suggesting that B cells contribute to the impaired antibody response to TD anti-

**Authorship note:** EJ and MT contributed equally to this work.

**Conflict of interest:** The authors have declared that no conflict of interest exists.



**Submitted:** October 25, 2019
**Accepted:** June 18, 2020
**Published:** August 6, 2020.

**Reference information:** *JCI Insight*. 2020;5(15):e134508. https://doi.org/10.1172/jci.insight.134508.

gens in DOCK8 deficiency (20), less is known about the role of T cells. We show that mice with selective DOCK8 deficiency in T cells mount poor IgG antibody responses to TD antigens, and have impaired GC formation and reduced numbers of GC B cells despite normal numbers of Tfh cells that are able to normally drive B cell differentiation in vitro. We demonstrate that activated DOCK8-deficient T cells have impaired LFA-1 activation and defective migration into GCs.

## Results

*DOCK8 expression in T cells is essential for a normal IgG antibody response to TD antigens*. *Dock8*$^{-/-}$ and *Cd4-Cre*$^{Tg}$*Dock8*$^{fl/fl}$ mice, which lack DOCK8 only in T cells (Supplemental Figure 1A; supplemental material available online with this article; https://doi.org/10.1172/jci.insight.134508DS1), and their controls were immunized in the hocks with the TD antigen TNP-KLH (2,4,6-trinitrophenyl–keyhole limpet hemocyanin). Serum anti-TNP IgG, but not IgM, antibody titers were significantly decreased in *Dock8*$^{-/-}$ and *Cd4-Cre*$^{Tg}$*Dock8*$^{fl/fl}$ mice (Figure 1A and Supplemental Figure 1B). Serum anti-TNP IgE antibody titers and IgE levels were not significantly different in *Cd4-Cre*$^{Tg}$*Dock8*$^{fl/fl}$ mice and their controls (Supplemental Figure 1C). This may be explained by known differences in the differentiation of B cells into IgE- versus IgG-secreting plasma cells (21). CD4$^+$ T cells from TNP-KLH–immunized *Cd4-Cre*$^{Tg}$*Dock8*$^{fl/fl}$ mice proliferated and secreted IL-2 and IFN-γ normally in response to in vitro stimulation with KLH, demonstrating that they did not have a global activation defect (Supplemental Figure 1, D and E).

The decreased IgG antibody response of *Cd4-Cre*$^{Tg}$*Dock8*$^{fl/fl}$ mice to TNP-KLH was not specific for either antigen or route of immunization. *Cd4-Cre*$^{Tg}$*Dock8*$^{fl/fl}$ mice had a decreased 4-hydroxy-3-nitrophenylacetyl hapten (anti-NP) IgG antibody response to hock immunization with NP-OVA in alum (Figure 1B), as well as decreased TNP- and OVA-specific IgG antibody responses to i.p. immunization with TNP-KLH and OVA in alum (Figure 1B). These findings demonstrate that DOCK8 expression in T cells is important for the IgG antibody response to TD antigen.

*DOCK8 expression in T cells is essential for normal GC formation and generation of GC B cells*. GC development in draining LNs is first observed 2–3 days following immunization with TD antigen (12), and a mature GC forms by approximately 7 days (22). GC formation in the popliteal LN of *Cd4-Cre*$^{Tg}$*Dock8*$^{fl/fl}$ mice was assessed by immunofluorescence microscopy on day 10 after immunization in the hock with TNP-KLH in alum. GCs were significantly reduced in size in the LNs of *Cd4-Cre*$^{Tg}$*Dock8*$^{fl/fl}$ mice compared with *Cd4-Cre*$^{Tg}$ controls (Figure 2A). GCs are important for the formation of high-affinity IgG antibody (23). Levels of high-affinity antibodies against TNP were decreased in *Cd4-Cre*$^{Tg}$*Dock8*$^{fl/fl}$ mice compared with *Cd4-Cre*$^{Tg}$ controls 14 days after immunization with TNP-KLH (Figure 2B), suggesting that the smaller GCs formed in *Cd4-Cre*$^{Tg}$*Dock8*$^{fl/fl}$ mice were less efficient in promoting antibody affinity maturation.

There was a significant decrease in the percentage and number of mature GC B cells in the draining LNs of *Cd4-Cre*$^{Tg}$*Dock8*$^{fl/fl}$ mice (Figure 2C). Surface expression of GL7 and FAS on GC B cells was significantly reduced in *Cd4-Cre*$^{Tg}$*Dock8*$^{fl/fl}$ mice (Figure 2D). Surface levels of GL7 and FAS on GC B cells correlate with their maturation state (24); their reduction on GC B cells from *Cd4-Cre*$^{Tg}$*Dock8*$^{fl/fl}$ mice may be due to a block in GC B cell maturation or could reflect an artificial lowering of the MFI due to contamination of the few "true" GC B cells with non-GC B cells. GC B cells are highly proliferating cells and express BCL6 (25, 26). Intracellular FACS staining revealed that the percentage of proliferating BCL6$^+$Ki-67$^+$ B cells in draining LNs was severely reduced in *Cd4-Cre*$^{Tg}$*Dock8*$^{fl/fl}$ mice (Figure 2E). However, intracellular expression of BCL6 and Ki-67 in BCL6$^+$ B cells was not affected (Figure 2F). These data indicate that DOCK8 expression in T cells is critical for supporting the differentiation and/or maintenance of GC B cells.

Differentiation of GC B cells following immunization with TD antigen is preceded by the generation of FAS$^{int}$GL7$^{lo}$IgD$^{hi}$CCR6$^{hi}$ pre-GC B cells in the interfollicular regions of the LN driven by the interaction between antigen-specific T and B cells. Pre-GC B cells subsequently enter the follicles to form GC B cells that upregulate FAS and GL7 expression and downregulate CCR6 and IgD expression. The percentage of pre-GC B cells in draining LNs peaks on day 2 after immunization (24, 27–29). The percentage of pre-GC B cells among B220$^+$ B cells in the draining LNs on day 2 after immunization with TNP-KLH was comparable in *Cd4-Cre*$^{Tg}$*Dock8*$^{fl/fl}$ mice and controls (Supplemental Figure 2 and Figure 2G). To fully examine pre-GC development, use of hapten-specific B cells would be required. Furthermore, the proliferation of pre-GC B cells, as indicated by the MFI of Ki-67 staining, was also similar in the 2 groups (Figure 2G). These results suggest that impaired generation of GC B cells in *Cd4-Cre*$^{Tg}$*Dock8*$^{fl/fl}$ mice is not secondary to defective T–B cell interactions in the interfollicular area of the LN.

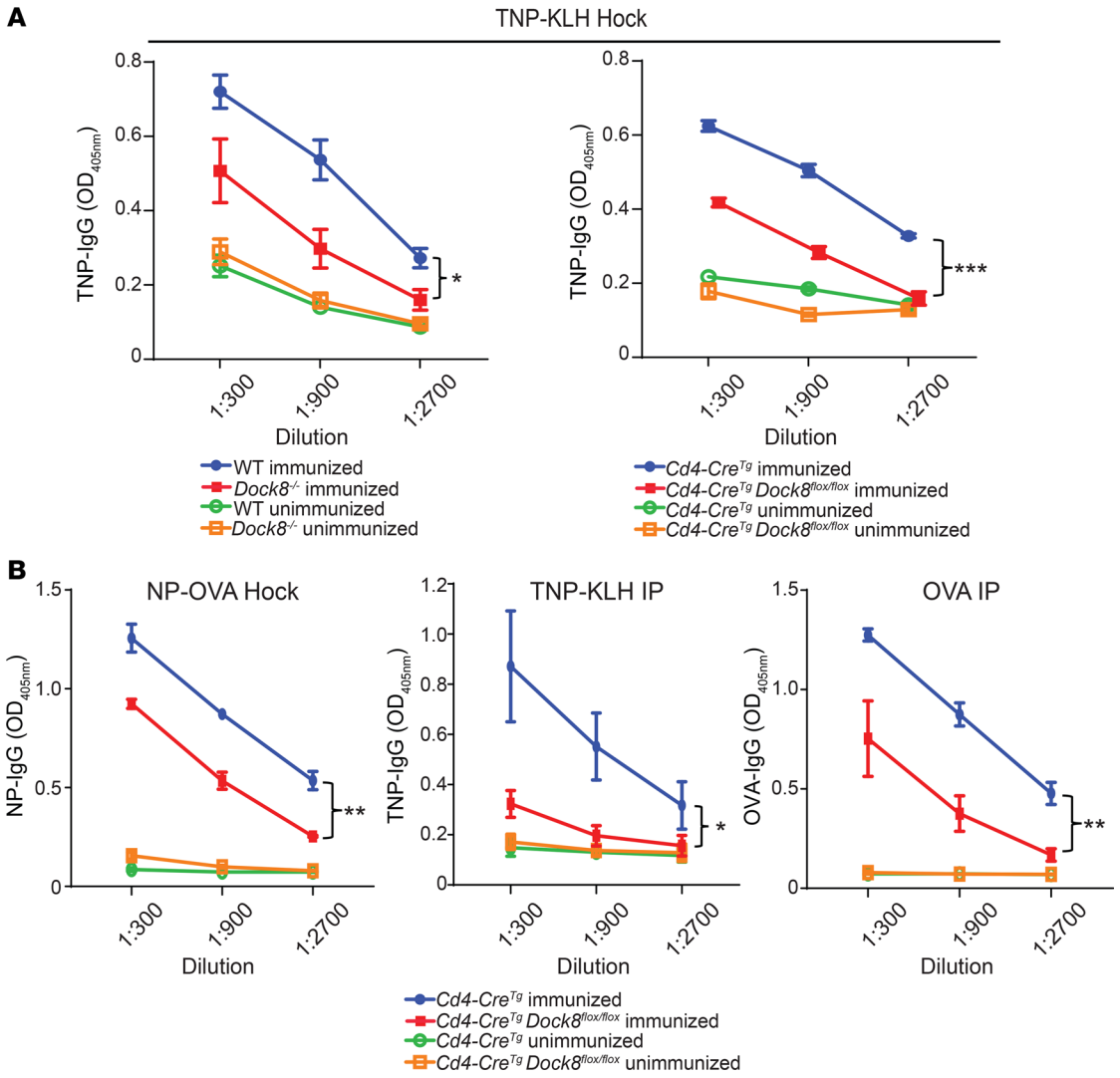


**Figure 1. Impaired antibody responses to TD antigens in *Cd4-Cre$^{Tg}$Dock8$^{fl/fl}$* mice.** (**A**) TNP-specific serum IgG levels on day 0 (unimmunized) and day 21 (immunized) from *Dock8$^{-/-}$* (left), *Cd4-Cre$^{Tg}$Dock8$^{fl/fl}$* mice (right), and controls after immunization in the bilateral hocks with TNP-KLH. (**B**) NP-specific serum IgG, TNP-specific serum IgG, and OVA-specific serum IgG measured on day 0 and day 21 after immunization of *Cd4-Cre$^{Tg}$Dock8$^{fl/fl}$* mice and controls with NP-OVA in the hocks, TNP-KLH i.p., or OVA i.p. **A** and **B** show data from 1 representative experiment of 2. *n* = 4–5 mice/group. Data are presented as mean ± SEM. **P* < 0.05, ***P* < 0.01, ****P* < 0.001 by ANOVA.

*DOCK8 expression in T cells is dispensable for the generation of Tfh cells and their in vitro function*. Given the reduced number of GC B cells in *Cd4-Cre$^{Tg}$Dock8$^{fl/fl}$* mice immunized with TNP-KLH (Figure 2C), we examined Tfh cells in draining LNs 7 days after immunization. The percentages and numbers of CXCR5$^{+}$PD-1$^{+}$ Tfh cells were similar in *Cd4-Cre$^{Tg}$Dock8$^{fl/fl}$* mice and controls (Figure 3A). T follicular regulatory (Tfr) cells express Tfh markers as well as FOXP3 and downregulate the GC reaction (30). The Tfr/Tfh cell ratio in draining LNs was also comparable in immunized *Cd4-Cre$^{Tg}$Dock8$^{fl/fl}$* mice and controls (Figure 3B).

We next investigated whether DOCK8-deficient Tfh cells have an altered phenotype that may impair their function. The Tfh cell markers CXCR5, PD-1, and ICOS not only help define the Tfh cell population, but are important for Tfh cell recruitment to the follicle, expression of BCL6, and survival (3–6, 31–33). Surface expression of CXCR5 and PD-1 was normal but ICOS expression was slightly decreased in Tfh cells from *Cd4-Cre$^{Tg}$Dock8$^{fl/fl}$* mice compared with controls (Figure 3C). Intracellular expression of BCL6 in Tfh cells was similar in the 2 groups (Figure 3D). Tfh cells highly express CD40L and signaling lymphocyte activation molecule (SLAM) family members (34–36). CD40L is important for the generation of GC reactions (37), while SLAM (CD150) is crucial for cytokine production by Tfh cells (36). Moreover, the SLAM family member CD84 plays a critical role stabilizing Tfh–B

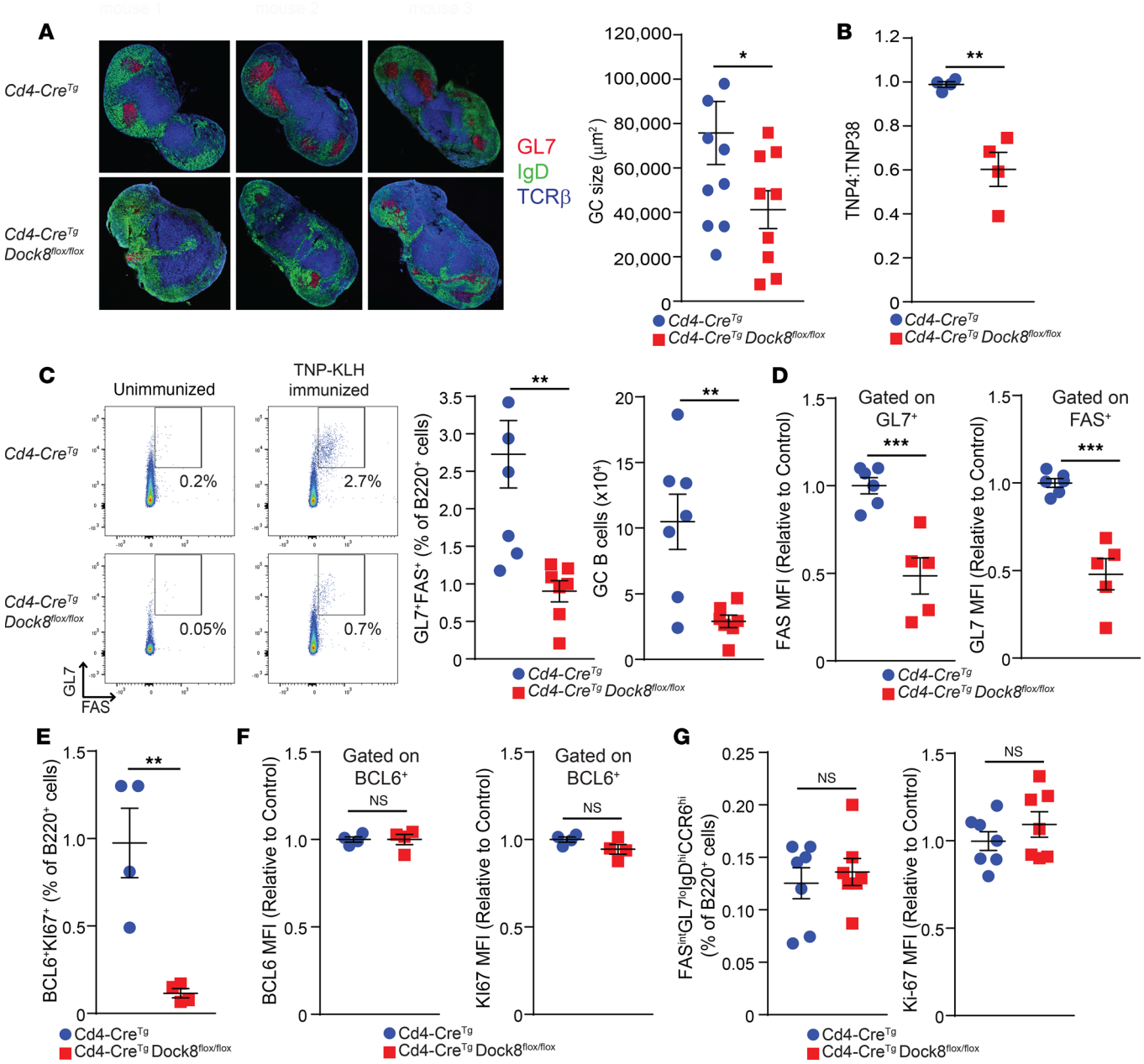


**Figure 2. *Cd4-Cre$^{Tg}$Dock8$^{fl/fl}$* mice have a marked reduction in GC B cells after immunization with TD antigen.** Draining LNs from *Cd4-Cre$^{Tg}$Dock8$^{fl/fl}$* and control mice immunized in the hocks with TNP-KLH were examined on day 2 for pre-GC B cells, on day 7 for GC B cells, and on day 10 for GC size. (**A**) Representative immunofluorescence photomicrograph of popliteal LNs (left). B cell follicles (IgD$^+$) are in green, GCs (GL7$^+$) in red, and the T cell zones (TCRβ$^+$) in blue. Images are at ×20 magnification. Quantification of GC size (right). $n$ = 4–5 mice/group in 2 pooled independent experiments. ANOVA; *$P$ < 0.05. (**B**) TNP-specific IgG affinity determined on day 14 after immunization. $n$ = 4 mice/group. Results are representative of 2 independent experiments. (**C**) Representative flow cytometry plots, and percentages and numbers of FAS$^+$GL7$^+$ GC B cells in draining LNs. $n$ = 7 mice/group. (**D**) MFI of surface FAS and GL7 by B220$^+$GL7$^+$ and B220$^+$FAS$^+$ cells, respectively. $n$ = 5–6 mice/group. (**E**) Percentages of BCL6$^+$KI-67$^+$ B cells in draining LNs. $n$ = 4 mice/group. (**F**) MFI of BCL6 and KI-67 (right) in BCL6$^+$ B cells. $n$ = 4 mice/group. (**G**) Percentage of FAS$^{int}$GL7$^{lo}$IgD$^{hi}$CCR6$^{hi}$ pre-GC B cells and MFI of KI-67 in pre-GC B cells. $n$ = 7 mice/group from 2 pooled experiments. **D–F** show a representative experiment of 3. Data are presented as mean ± SEM. Student's $t$ test; *$P$ < 0.05, **$P$ < 0.01, ***$P$ < 0.001.

cell interactions (35, 36), and the SLAM-associated adapter protein (SAP) is required for late-stage Tfh cell differentiation, Tfh–B cell conjugate formation, and GC development (35, 38–40). Surface expression of CD40L, the SLAM molecules CD150 and CD84, as well as mRNA levels of *Sh2d1a* (encoding SAP) were comparable in Tfh cells from the 2 groups (Figure 3E). Furthermore, intracellular staining revealed similar percentages of IL-4– and IL-21–expressing Tfh cells in *Cd4-Cre$^{Tg}$Dock8$^{fl/fl}$* mice and controls (Supplemental Figure 3A and Figure 3F).

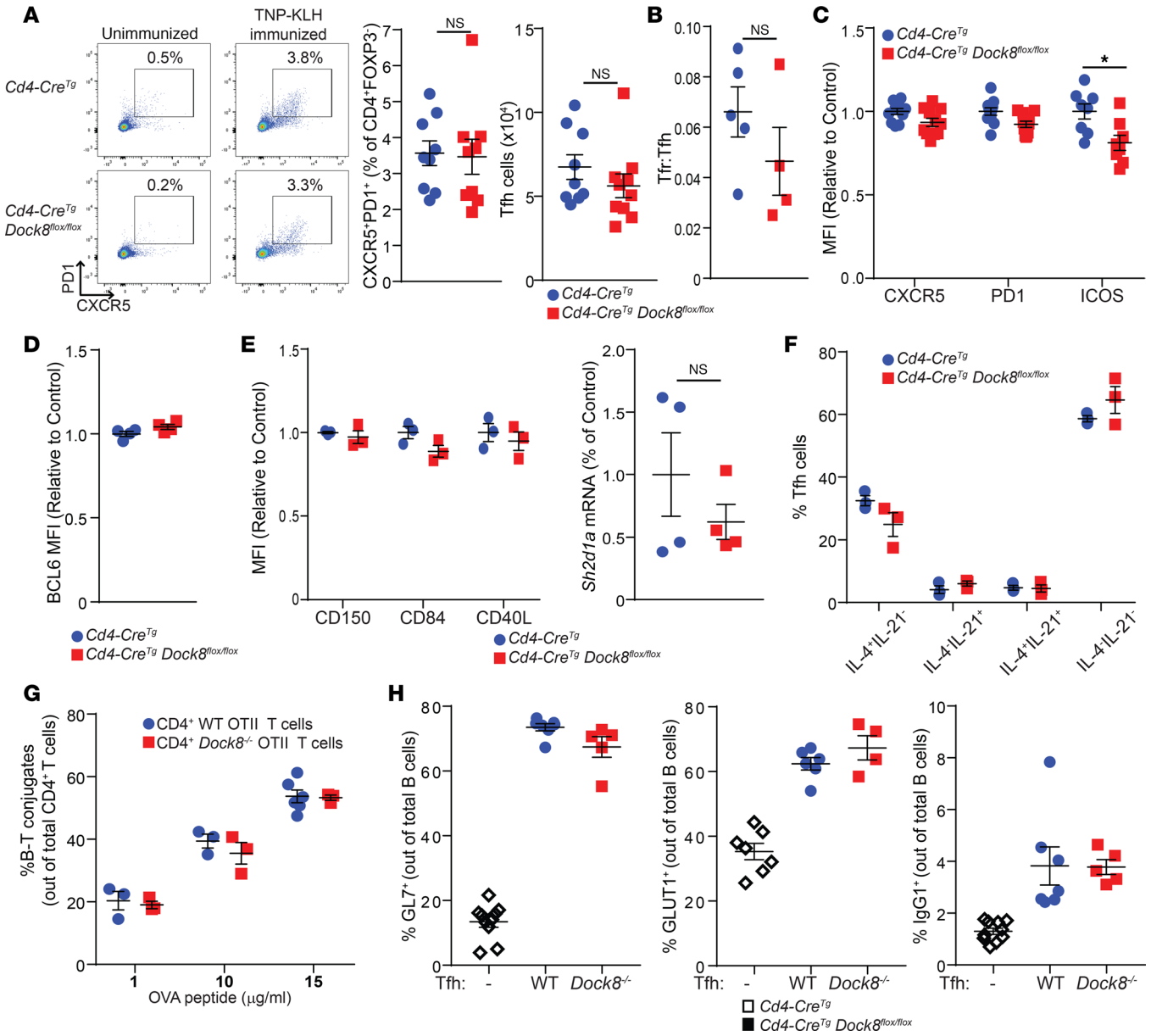


**Figure 3. *Cd4-Cre$^{Tg}$Dock8$^{fl/fl}$* mice have a normal Tfh percentage and phenotype after immunization with TD antigen.** *Cd4-Cre$^{Tg}$Dock8$^{fl/fl}$* mice and controls were immunized with TNP-KLH in the hock. Draining LNs were analyzed 7 days after immunization. (**A**) Representative FACS plots, and percentages and numbers of CXCR5$^+$PD-1$^+$ Tfh cells. Pooled results from 3 individual experiments; $n$ = 9 mice/group. (**B**) Ratio of Tfr to Tfh cells. (**C**) MFI of CXCR5, PD-1, and ICOS expression by Tfh cells. (**D**) Intracellular BCL6 expression by Tfh cells. (**E**) MFI of CD150, CD84, and CD40L expression by Tfh cells (left). qPCR analysis of *Sh2d1a* mRNA expression in sorted Tfh cells (right). Results are expressed as fold increase in *Sh2d1a* mRNA/β2 microglobulin mRNA ratio relative to control. (**F**) Intracellular expression of IL-4 and IL-21 by Tfh cells stimulated for 4 hours with phorbol-12,13-dibutyrate and ionomycin. (**G**) Percentage of B–T cell conjugates of total CD4$^+$ T cells isolated from *Dock8$^{-/-}$* OT II and WT OT II mice incubated for 3 hours with LPS-stimulated WT B cells pulsed with $OVA_{323-339}$. (**H**) Sorted CD4$^+$ICOS$^+$CXCR5$^+$CD25$^-$CD19$^-$ Tfh cells from the draining LNs were incubated with CD19$^+$ B cells sorted from the LNs of WT mice in the presence of soluble anti-CD3 and anti-IgM. Cell surface expression of GL7, GLUT1, and IgG1 by B cells after 6 days in culture is shown. Results in **B**–**H** are representative of 3 independent experiments. Data are presented as mean ± SEM. Student's $t$ test; *$P < 0.05$.

We conducted an unbiased screen for differences in gene expression between DOCK8-deficient and WT Tfh cells. We established a >1.5-fold change with $P < 0.05$ as the threshold for a significant change in gene expression. RNA-Seq analysis revealed that expression of 18 genes was significantly downregulated in Tfh cells from *Cd4-Cre$^{Tg}$Dock8$^{fl/fl}$* mice compared with controls. These included genes encoding proteins involved in cell-cell interactions — CD96, CD73 (*Nt5e*), Sirpa, Cldn25, and Ifitm3 (41–45); and in cell motility and shape — Myo1e, Actg2, and Klhl4 (46–48) (Supplemental Figure 3B). There was also reduced expression of genes encoding the chemokine CCL8, ceramide synthase 4 (*Cers4*), and galectin-like protein

(*Lgalsl*) (49, 50). Only 4 genes were expressed at a higher level in Tfh cells from *Cd4-Cre$^{Tg}$Dock8$^{fl/fl}$* mice. These included *B4galt4*, *Bckdhb*, *Tbc1d23*, and *Timmdc1*, all encoding intracellular proteins with unknown relevance to Tfh cell function (Supplemental Figure 3B). Notably, there were no significant differences in expression of *Il4*, *Il13*, *Il5*, or *Il21* in Tfh cells from *Cd4-Cre$^{Tg}$Dock8$^{fl/fl}$* mice and controls (Supplemental Figure 3B). Decreased expression of genes important for cell-cell interaction and cell motility in Tfh cells may have contributed to defective GC formation in *Cd4-Cre$^{Tg}$Dock8$^{fl/fl}$* mice.

Conjugate formation between T cells and B cells presenting cognate antigen allows these B cells to effectively compete for cytokines crucial for their differentiation (51). The ability of DOCK8-deficient T cells to form conjugates with WT B cells in vitro was examined. OVA peptide–specific CD4$^+$ T cells were purified from *Dock8$^{-/-}$* OT II mice and OT II controls and incubated for 3 hours with LPS-activated WT B cells pulsed with $OVA_{329–337}$ peptide. Conjugate formation was assessed by flow cytometry. DOCK8-deficient CD4$^+$ T cells and WT CD4$^+$ T cells had similar percentages of conjugate formation with WT B cells (Figure 3G). Similarly, DOCK8-deficient CD4$^+$ T cells had intact conjugate formation when incubated with WT bone marrow–derived DCs (BMDCs) pulsed with OVA peptide (Supplemental Figure 3C). Thus, in the absence of spatial constraints, short-term in vitro conjugate formation between DOCK8-deficient T cells and antigen-presenting cells (APCs; both B cells and DCs) was intact.

Next, the ability of DOCK8-deficient Tfh cells to promote in vitro B cell differentiation was examined. WT and DOCK8-deficient CD4$^+$ICOS$^+$CXCR5$^+$CD25$^-$CD19$^-$ Tfh cells were sorted from the draining LNs of TNP-KLH immunized mice and cultured with WT CD19$^+$ B cells in the presence of anti-CD3 and anti-IgM. After 6 days in culture, B cell surface markers were examined by flow cytometry. WT and DOCK8-deficient Tfh cells were comparably potent in inducing the expression of GL7 and the glucose transporter GLUT1 on B cells (Figure 3H). In addition, a comparable percentage of B cells was surface IgG1$^+$ (sIgG1$^+$) after stimulation with DOCK8-deficient Tfh cells and WT Tfh cells (Figure 3H). These data demonstrate that DOCK8-deficient Tfh cells were normal in number, and able to secrete cytokines and provide help for the generation of GC B cells in vitro.

*DOCK8-deficient T cells localize poorly to the GC, have impaired adhesion to ICAM-1, and fail to activate LFA-1 following TCR/CD3 ligation*. Tfh cell migration into the B cell follicle results in GC formation (1). GCs from draining LNs of immunized *Cd4-Cre$^{Tg}$Dock8$^{fl/fl}$* mice had fewer T cells than those from control mice (Supplemental Figure 4A). This prompted us to investigate whether DOCK8-deficient Tfh cells properly localize within the GC. CD4$^+$ T cells from CD45.2$^+$ *Dock8$^{-/-}$* OT II mice or OT II controls were adoptively transferred into CD45.1$^+$ recipients. Recipients were immunized the day after in the hock with NP-OVA, and draining LNs were examined 9 days later. GC area was comparable in recipients of DOCK8-deficient T cells and recipients of WT T cells (Supplemental Figure 4B), and endogenous CD45.1$^+$ T cells made up 59%–62% of the Tfh cells that developed regardless of whether DOCK8-deficient or WT CD45.2$^+$ T cells were transferred. This reflects the intact ability of the WT recipients to mount a GC reaction. Comparable numbers of CD45.2$^+$ T cells from *Dock8$^{-/-}$* donors and WT donors were found in the recipients' LNs (Figure 4A). The percentage of CD45.2$^+$ donor cells that developed into Tfh cells was comparable (Supplemental Figure 4C). In contrast, the percentage of donor CD45.2$^+$ T cells in the follicle that localized to the GC was significantly reduced in recipients of *Dock8$^{-/-}$* T cells compared with control T cells (Figure 4B). Our results suggest that antigen activated DOCK8-deficient T cells had impaired ability to migrate into the GC.

Tfh cells migrate toward CXCL13 produced by stromal cells in B cell follicles (6). Expression of the CXCL13 receptor CXCR5 was comparable in Tfh cells from *Cd4-Cre$^{Tg}$Dock8$^{fl/fl}$* mice and controls (Figure 3C). To examine the ability of Tfh cells to migrate in response to CXCL13, we immunized *Dock8$^{-/-}$* OT II and WT OT II mice in the hocks and i.p. with NP-OVA in alum to generate CXCR5$^+$ CD4$^+$ T cells. Ten days after immunization, CD4$^+$ T cells were isolated from the spleen and draining LNs. Approximately 40%–45% of the cells in the CD4$^+$ T cell preparation were CXCR5$^+$ from both *Dock8$^{-/-}$* and control mice. We found no significant difference in the ability of *Dock8$^{-/-}$* and control CD4$^+$ T cells to migrate in response to CXCL13 in a Transwell assay (Supplemental Figure 4D). This suggests that *Dock8$^{-/-}$* T cells had an intact CXCR5/CXCL13 axis.

Interaction between LFA-1, highly expressed on Tfh cells, and ICAM-1/2 on B cells is important for Tfh cell migration into GCs (7, 9). Following TCR ligation, LFA-1 undergoes a rapid conformational change to an activated form with high affinity for ICAMs (52, 53). LFA-1 surface expression was comparable in WT and DOCK8-deficient murine CD4$^+$ T cells (Figure 4C). However, anti-CD3–activated CD4$^+$ T cells from *Dock8$^{-/-}$* mice demonstrated significantly decreased binding to immobilized ICAM-1–Fc under

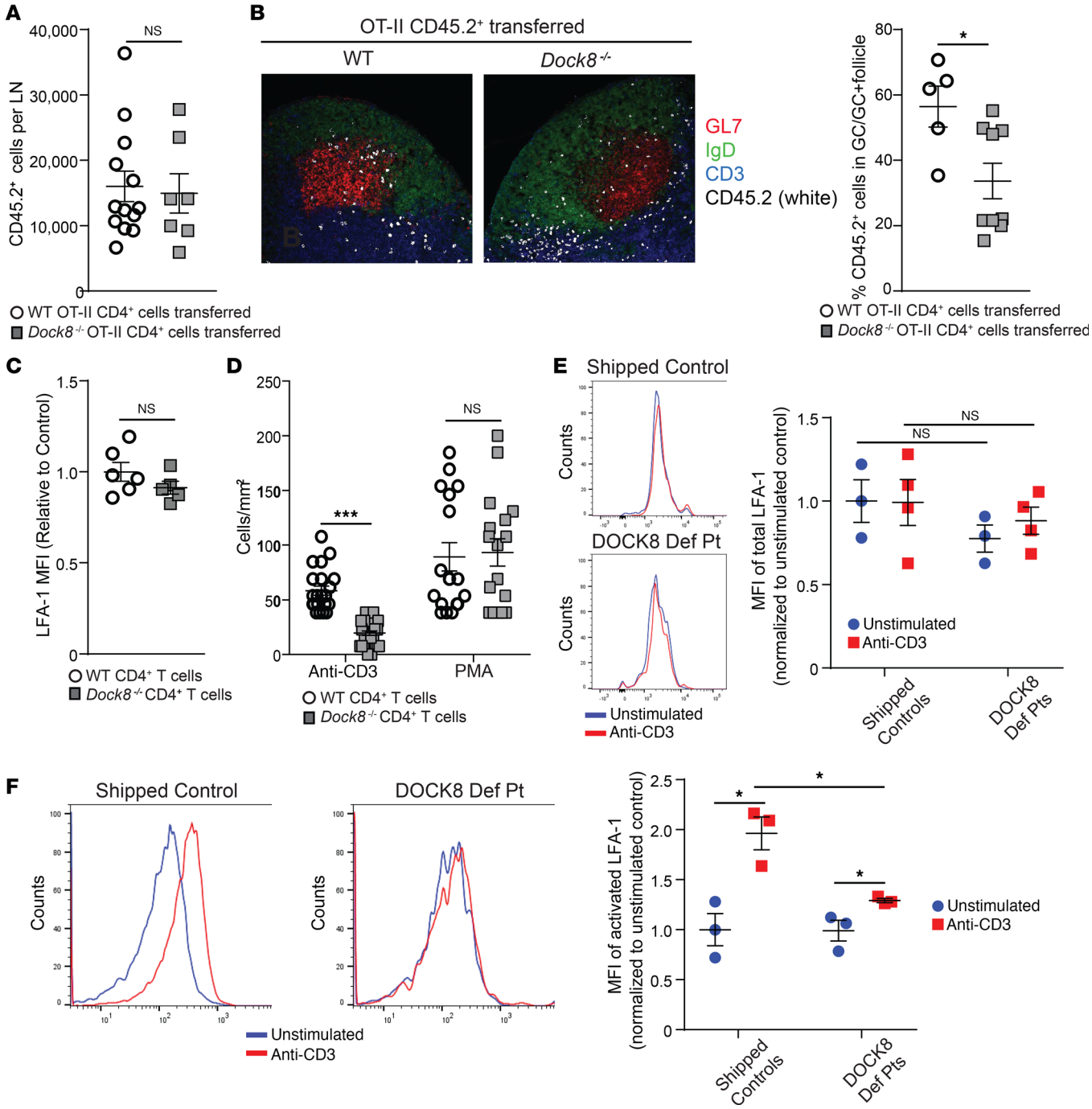


**Figure 4. DOCK8-deficient CD4⁺ T cells have decreased migration into GCs and impaired activation of LFA-1.** (**A** and **B**) CD4⁺CD45.2⁺ OT II WT or DOCK8-deficient T cells were adoptively transferred into CD45.1⁺ WT mice. Recipients were immunized with NP-OVA in the hock, and popliteal LNs were analyzed on day 9 after immunization. (**A**) The number of OT II CD45.2⁺ T cells found in the draining LNs of recipient mice was analyzed by flow cytometry. (**B**) Localization within the draining LNs of transferred CD4⁺CD45.2⁺ OT II WT or DOCK8-deficient T cells was examined by immunofluorescence microscopy. Representative photomicrographs at ×20 magnification: B cell follicles (IgD⁺) are in green, GCs (GL7⁺) in red, CD45.2⁺ T cells in white, and T cell zones (CD3⁺) in blue. Percentage of CD45.2⁺ in GCs relative to total CD45.2⁺ cells in GC plus the surrounding follicle normalized to the GC and follicle area. $n$ = 5 mice/group. (**C**) MFI of total surface LFA-1 expression on CD4⁺ T cells from *Dock8*$^{-/-}$ mice and WT controls. (**D**) Number of adherent CD4⁺ T cells, stimulated with anti-CD3 or PMA from *Dock8*$^{-/-}$ mice and controls, to ICAM-1 10 minutes after application to a flow chamber with a flow rate of 0.75 dynes/cm². Five fields were examined per slide. (**E**) Representative histograms and MFI of LFA-1 surface expression by unstimulated and anti-CD3–stimulated CD4⁺ T cells from DOCK8-deficient patients (DEF Pt) and healthy shipped controls ($n$ = 3/group). MFI values were normalized to the mean value of shipped controls. (**F**) Representative histograms and MFI of activated LFA-1 expression by unstimulated and anti-CD3–stimulated CD4⁺ T cells from DOCK8-deficient patients and healthy shipped controls ($n$ = 3/group). MFI values were normalized to the mean value of unstimulated shipped controls. Results in **C** and **D** are from 3 independent experiments, each with 3 mice/group. Data in **A**–**F** are presented as mean ± SEM. In **A**–**C**, Student's $t$ test; *$P$ < 0.05. In **D**–**F**, 1-way ANOVA with Tukey's multiple comparisons; *$P$ < 0.05, **$P$ < 0.01, ***$P$ < 0.001.

physiologic flow conditions (Figure 4D). Following stimulation with PMA, which bypasses the TCR, adhesion to ICAM-1 was comparable in DOCK8-deficient and WT $CD4^+$ T cells (Figure 4D).

Using a monoclonal antibody (mAb m24) that selectively recognizes the active conformation of LFA-1 on human cells, we examined the ability of T cells from DOCK8-deficient patients with homozygous *DOCK8* mutations that abrogated protein expression (see Methods) to activate LFA-1 following TCR/CD3 ligation. Surface expression of LFA-1 was comparable in unstimulated $CD4^+$ T cells from the patients and control donors and remained unchanged after 30 minutes of anti-CD3 stimulation (Figure 4E). Following TCR/CD3 ligation, $CD4^+$ T cells from controls demonstrated a significant increase in activated LFA-1 on their surface (Figure 4F). Activated $CD4^+$ T cells from patients demonstrated a small increase in activated LFA-1, but the level was significantly lower than in control cells (Figure 4F). These results suggest that decreased T cell LFA-1 activation, leading to a defective interaction with ICAM/2 on B cells, may have impaired migration of DOCK8-deficient Tfh cells into GCs.

## Discussion

We demonstrate that DOCK8 expression in T cells is critical for the migration of Tfh cells into GCs and thereby for normal GC formation, generation of GC B cells, and production of high-affinity IgG antibodies to TD antigens.

Recently, Gowthaman et al. reported that *Cd4-Cre$^{Tg}$Dock8$^{fl/fl}$* mice immunized with NP-OVA plus LPS intranasally demonstrate reduced IgG antibody levels with decreased affinity. However, in contrast to our findings, serum IgE levels were elevated, GCs were normal in size, and GC B cells were not reduced (54). Immunizing our *Cd4-Cre$^{Tg}$Dock8$^{fl/fl}$* mice using the same protocol yielded similar results (data not shown). LPS is an adjuvant that activates B cells and innate cells via TLR4 and promotes Th1 responses at high doses and Th2 responses at low doses (55, 56). In contrast, alum, the adjuvant we used, is commonly used in human vaccines and promotes type 2 cytokine production by innate cells including ILC2s and NKT cells (57–60). Differences in the mechanisms of action of these adjuvants, as well as the route of immunization, may underlie the differences between the study by Gowthaman et al. and ours.

Although required for normal GC formation, DOCK8 expression in T cells was not required for the generation of Tfh cells. DOCK8 expression also was not required for Tfh cells to express cytokines and surface molecules important for GC formation, the formation of antigen-dependent conjugates with B cells or DCs, or in vitro Tfh-driven B cell differentiation into GC B cells. The primary defect observed in DOCK8-deficient Tfh cells was their reduced capacity to migrate into GCs. DOCK8 deficiency may affect signaling downstream of chemoattractants. In addition, normal expression of SLAM family members by DOCK8-deficient T cells does not rule out defective signaling by these molecules, which would contribute to the defective migration of these cells into GCs and impaired generation of GC B cells.

A major finding of our study is that DOCK8 is essential for activation of LFA-1 following TCR ligation and for the ability of TCR-activated T cells to bind to ICAM-1. Since the interaction of LFA-1 on Tfh cells with ICAM-1/2 on B cells is important for GC formation (61), defective LFA-1 activation in T cells likely contributes to the defective GC formation in DOCK8 deficiency. Diminished binding to ICAM-1 by activated DOCK8-deficient total T cells, $CD8^+$ T cells, Tregs, and B cells has been previously noted (20, 62–64).

DOCK8 exists in a macromolecular complex with Wiskott-Aldrich syndrome protein (WASP) and Talin (63, 65). Downstream of antigen receptor engagement, DOCK8 loads CDC42 with GTP, leading to WASP activation (63). WASP activation is important for LFA-1 polarization and function (66, 67). TCR ligation also causes the DOCK8-associated protein Talin to bind to the β chain of integrins, which is critical for LFA-1 activation (65, 68). Either LFA-1 blockade or deletion of Talin-1 blocks the generation of Tfh cells (69). Thus, both WASP and Talin may mediate DOCK8-dependent LFA-1 activation following TCR.

It is noteworthy that DOCK8 deficiency in T cells affects the generation of GC B cells, but not of Tfh cells. The residual LFA-1 activation and adhesion to ICAM-1–expressing cells in antigen-activated DOCK8-deficient T cells may allow sufficient contact between T and B cells to generate normal numbers of Tfh cells, but may not be sufficiently strong and/or long-lasting to allow normal Tfh cell migration into GCs. Impaired migration of Tfh cells into GCs results in compromised GC B cell development and defective IgG antibody production and affinity maturation in DOCK8 deficiency.

## Methods

*Mice*. *Dock8*$^{-/-}$ and *Dock8*$^{fl/fl}$ mice are described in refs. 62, 63. *Dock8*$^{fl/fl}$ mice were mated with *Cd4-Cre*$^{Tg}$ mice (Taconic) to generate *Cd4-Cre*$^{Tg}$*Dock8*$^{fl/fl}$ mice. *Dock8*$^{-/-}$ mice were bred with OT II mice (Charles River) to generate *Dock8*$^{-/-}$ OT II mice. Both female and male mice were studied. All mice were kept in a specific pathogen–free environment.

*Patients*. Blood samples were obtained from healthy volunteers and 4 DOCK8-deficient patients with homozygous mutations in *DOCK8* (c.3191delA, c.4826_4827delAC, and c.3787delA) that abolish DOCK8 expression. Two of the DOCK8-deficient patients were female, and 2 were male. All patients were between 5 and 9 years old.

*Immunoblotting*. Total B cells and T cells were purified from the spleens of *Cd4-Cre*$^{Tg}$*Dock8*$^{fl/fl}$ and controls using magnetic beads (Miltenyi Biotec). Cells were lysed in 1% Triton buffer (150 mM NaCl, 25 mM Tris-Cl, pH 7.5, 5 mM EDTA) containing complete protease inhibitors (Roche). Cell lysates were separated by SDS-PAGE, transferred to nitrocellulose, and immunoblotted with mAbs against DOCK8 (H159, Santa Cruz Biotechnology) and β-actin (ab8226, Abcam).

*Immunizations*. Mice were immunized either i.p. or in the bilateral hocks with 10 μg TNP-KLH (Biosearch Technologies, T-5060), NP-OVA (Biosearch Technologies, N-5051), or OVA (MilliporeSigma) in alhydrogel adjuvant (vac-alu-250, InvivoGen), and boosted on day 14 with 2.5 μg antigen in adjuvant. Sera were collected on days 0, 14, and 21. To study pre-GC B cell, GC B cell, or Tfh cell generation, or GCs, we harvested draining LNs (inguinal and popliteal) on days 2, 7, or 10 from hock-immunized mice. To examine antibody affinity maturation, mice were immunized in the bilateral hocks with 1 μg TNP-KLH, and sera was collected on day 14.

*ELISAs*. For antigen-specific antibody responses, 96-well plates (Thermo Fisher Scientific) were coated overnight at 4°C with 10 μg/mL $TNP_4$-BSA (Biosearch Technologies), $TNP_{38}$-BSA (Biosearch Technologies), NP-BSA (Biosearch Technologies), or OVA (MilliporeSigma). Blocking was accomplished with 3% BSA in PBS. Serial dilutions of sera were applied to the plates overnight at 4°C. After washing, AP-conjugated goat anti-mouse IgG (Southern Biotech) was applied to the plates for 2 hours at room temperature. Bound secondary antibodies were detected by incubation with *p*-nitrophenyl phosphate (PNPP) substrate (MilliporeSigma). For detection of total serum IgE, 96-well plates were coated with anti-IgE (R35-72, BD Biosciences). For detection of total and TNP-specific IgE antibodies, biotin-conjugated rat anti-mouse IgE (R35-118, BD Biosciences) was applied to plates for 2 hours at room temperature. Bound secondary antibodies were detected with avidin-conjugated HRP (Thermo Fisher Scientific) and developed by incubation with TMB substrate (Thermo Fisher Scientific).

*Cellular proliferation and cytokine secretion*. Inguinal and popliteal LNs were harvested on day 21 from mice immunized in the hock with TNP-KLH. Cells were stained with CellTrace Violet (Life Technologies) and stimulated with the indicated concentrations of KLH antigen (374825, Calbiochem). After 24 and 72 hours in culture, IL-2 and IFN-γ content was measured by ELISA according to the manufacturer's instructions (Thermo Fisher Scientific). Proliferation was assessed by flow cytometry on day 5 of culture.

*Flow cytometry*. Single-cell suspensions were made of the draining LNs. For staining of surface molecules, cells were incubated on ice with fluorochrome-conjugated mAbs against CD3 (145-2c11), CD4 (GK1.5), CD8 (clone 53-6.7), GL7 (GL7), FAS (15A7), IgD (11-26c.2a), CCR6 (29-2L17), PD-1 (29F.1A12), ICOS (C398.4A), CD25 (PC61.5), CD40L (MR1), CD84 (mCD84.7), SLAM (TC15-12F12.2), CD19 (6D5) from BioLegend, B220 (RA3-6B2) from Thermo Fisher Scientific, and GLUT1 (EPR3915) from Abcam. For CXCR5 staining, biotinylated CXCR5 (SPRLC5, Thermo Fisher Scientific) was used, followed by streptavidin-PE or streptavidin–PE–Texas red (BioLegend). For intracellular staining with antibodies against FOXP3 (FJK-165), KI-67 (16A8), BCL6 (K112-91), and IgG1 (A85-1) from BioLegend, cells were fixed, permeabilized, and stained according to the manufacturer's directions (Thermo Fisher Scientific).

For intracellular cytokine staining, cells were stimulated with phorbol 12,13-dibutyrate and ionomycin (MilliporeSigma) in the presence of GolgiStop and GolgiPlug (BD Biosciences) for 4 hours. Cells were then fixed and permeabilized using a BD Biosciences Cytofix/Cytoperm kit and incubated with a fluorochrome-conjugated antibody against IL-4 (11B11, Thermo Fisher Scientific) and with recombinant human IL-21R Fc chimera protein (991-R2-100, R&D Systems), followed by Alexa Fluor 647 AffiniPure $F(ab')_2$ Fragment Goat Anti-Human IgG (109-606-008, Jackson ImmunoResearch Laboratories Inc.).

*LFA-1 expression on human T cells*. Human PBMCs were isolated from whole blood by Ficoll-Paque PLUS density gradient centrifugation (GE Healthcare). PBMCs were stimulated by incubation with

anti-CD3 (OKT3, Thermo Fisher Scientific), followed by cross-linking with goat anti-mouse IgG (115-006-072, Jackson ImmunoResearch Laboratories Inc.). Samples were stained with total LFA-1 (TS2/4), active LFA-1 (m24), CD4 (OKT4), and Zombie Violet viability dye, all from BioLegend.

All data were acquired on a BD LSRFortessa cell analyzer using FACSDiva software (BD Biosciences). Analyses were performed using FlowJo software (Tree Star Inc.).

*BMDC generation*. DCs were generated from WT mice. The femurs and tibias were isolated. BM cells were flushed from the marrow cavities. Red blood cells were lysed with ACK buffer. Bone marrow cells were cultured in media supplemented with 10 ng/mL GM-CSF and 10 ng/mL IL-4. After 6 days, the immature DCs were harvested and re-plated with 50 ng/mL LPS. Cells were harvested 24 hours later for use in in vitro conjugation assays.

*In vitro conjugation assays*. $CD4^+$ OT-II T cells were isolated from the spleens of *Dock8*$^{-/-}$ OT II mice or OT II controls using the Miltenyi Biotec $CD4^+$ T Cell Isolation Kit and stained with anti–mouse CD4–APC-Cy7 (RM45, BioLegend). B cells were isolated from WT spleens using magnetic beads (Miltenyi Biotec) and stimulated with 1 μg/mL LPS plus $OVA_{323–339}$ peptide (AnaSpec) for 3 hours, washed, and then stained with anti–mouse CD19 BV605 (6D5, BioLegend). OT II $CD4^+$ T cells ($5 \times 10^5$/well) and activated B cells ($2 \times 10^6$/well) were incubated for 3 hours at 37°C in 96-well U-bottom plates. To examine $CD4^+$ T cell conjugate formation with BMDCs, BMDCs were stimulated for 3 hours with $OVA_{323–339}$ peptide. OT II $CD4^+$ T cells ($2 \times 10^5$/well) and BMDCs ($1 \times 10^5$/well) were incubated for 3 hours at 37°C in 96-well U-bottom plates. Conjugate frequencies were enumerated by flow cytometry.

*In vitro stimulation assays*. For in vitro B cell stimulation assays with Tfh cells, *Cd4-Cre*$^{Tg}$*Dock8*$^{fl/fl}$ mice and controls were immunized with TNP-KLH in alhydrogel in the hock. Seven days later, popliteal and inguinal LNs were harvested. $CD4^+ICOS^+CXCR5^+CD25^-CD19^-$ Tfh cells were isolated by cell sorting. $3 \times 10^4$ WT or DOCK8-deficient Tfh cells were plated with $5 \times 10^4$ B cells (sorted as $CD19^+CD4^-$ cells from LNs of TNP-KLH–immunized *Cd4-Cre*$^{Tg}$ controls) along with 2 μg/mL soluble anti-CD3 (BioExcel) and 5 μg/mL anti-IgM (Jackson ImmunoResearch Laboratories Inc.). Assays were performed as described as previously described (70). Six days later, cell surface markers were analyzed by flow cytometry (described above).

*Quantitative analysis of gene expression*. Tfh cells were isolated by fluorescence sorting for $CD4^+CD19^-CD25^-CXCR5^+ICOS^+$ cells from draining LNs of mice immunized in the hock with TNP-KLH. RNA was isolated using an RNAeasy Plus Micro Kit (QIAGEN) according to the manufacturer's instructions.

Complementary DNA was reverse transcribed using an iScript cDNA Synthesis Kit (Bio-Rad) according to the manufacturer's instructions. Analysis of transcripts was performed with a commercial TaqMan primer/probe set against mouse *Sh2d1a* with *B2m* as a control (Thermo Fisher Scientific). Relative mRNA expression was quantified using the $2^{-\Delta\Delta Ct}$ method.

For RNA-Seq, RNA was isolated as described above from Tfh cells. Low-input mRNA libraries (Clontech SMARTer v4) were generated and sequenced on an illumina NS500 Single-End 75bp (SE75) by the Dana Farber Cancer Institute Molecular Biology Core Facility. TopHat was used to align reads to mouse genome (Mm9, National Center for Biotechnology Information [NCBI]), and high-throughput sequencing (HT-Seq) was used to estimate read counts. DEseq2 (Bioconductor, https://doi.org/doi:10.18129/B9.bioc.DESeq2) was used to normalize data and access differential gene expression with a $P$ value less than 0.05. Expression was normalized using the geometric mean for each gene. Heat maps were generated using Prism (GraphPad Software), and data are shown as $\log_2$ fold change relative to the geometric mean. All original RNA-Seq data were deposited in the NCBI's Gene Expression Omnibus database (GEO GSE154897).

*LN imaging*. LNs from immunized mice were frozen in Tissue-Tek O.C.T. Compound and cryosectioned. Sections were fixed with 4% PFA for 10 minutes, washed 3 times in PBS, blocked 45 minutes with 10% goat serum in PBS, and stained 1 hour with 1:100 antibodies in 2% BSA in PBS. For GC imaging, fluorochrome-conjugated antibodies against TCRβ (H57-597), IgD-FITC (11.26c.2), and GL7 (GL7) from BioLegend were used. After washing 3 times with PBS, stained sections were mounted with ProLong Diamond Antifade Mountant (Thermo Fisher Scientific). Images were acquired on a Zeiss Elyra PS.1 confocal microscope and analyzed with Imaris 8.4.1.

For adoptive transfer studies, $CD4^+$ T cells were isolated from the spleens and LNs of OT II and *Dock8*$^{-/-}$ OT II mice using magnetic beads (Miltenyi Biotec). $10 \times 10^6$ cells were injected i.v. into $CD45.1^+$ mice. Twenty-four hours later, recipient $CD45.1^+$ mice were immunized in the hock with NP-OVA. After 9 days, popliteal LNs were harvested and processed as described above. In addition to the antibodies noted above,

fluorochrome-conjugated antibodies to CD3 (17A2) and CD45.2 (clone 104) from BioLegend were used. Images were acquired using a Zeiss LSM 880 Upright Laser Scanning Confocal Microscope and analyzed using ImageJ (NIH). For quantification, $CD45.2^+$ cells were counted in the GC and surrounding follicle, and the percentages of $CD45.2^+$ T cells in the GCs among total $CD45.2^+$ cells in the GC plus follicle were calculated. Data were normalized by the area of GCs and follicles as described in ref. 71.

*Transwell migration to CXCL13*. $CD4^+$ T cells were isolated from spleens and draining LNs of OT II and *Dock8*$^{-/-}$ OT II mice immunized i.p. and in the hock with NP-OVA plus alum using magnetic beads (Miltenyi Biotec). $1 \times 10^5$ $CD4^+$ T cells were applied to the upper chambers of a 5-μm-pore 96-well plate. CXCL13 was added to the bottom chamber in media with 1% FCS at concentrations of 0, 500, and 1000 ng/mL.

*T cell adhesion to immobilized ICAM1 under laminar shear flow conditions*. Live-cell imaging of $CD4^+$ T cells adhesion was recorded by a video camera coupled to a Nikon TE2000 inverted microscope equipped with a 20×/0.75 NA phase contrast objective and VideoLab software (Mitov) (72, 73). *Dock8*$^{-/-}$ and WT $CD4^+$ T cells were activated with anti-CD3 cross-linking or PMA for 20 minutes. Cells ($5 \times 10^5$ cells were suspended in 100 μL PBS) were flowed across immobilized 20 μg/mL ICAM-1–Fc in the presence of 250 ng/mL SDF-1α at a shear stress of 0.75 dynes/cm$^2$ (73). $CD4^+$ cell adhesion was determined in 5 separate fields for 1 minute and reflects accumulation of adherent cells.

*Statistics*. Comparisons were analyzed for statistical significance using unpaired 2-tailed Student's *t* test, 1-way ANOVA with Tukey's multiple-comparison tests, and 2-way ANOVA to determine the *P* value using Prism software (GraphPad Software). A *P* value less than 0.05 was considered significant. Germinal center size responses were fit to a linear mixed-effects model in R (version 3.4.2, https://www.r-project.org/) and tested using ANOVA. Genotype was specified as a fixed effect; immunization batch, individual, and LN were treated as nested random effects.

*Study approval*. All mouse studies were approved and performed in accordance with the Boston Children's Hospital Institutional Animal Research and Care Committee. Parents or guardians gave written informed consent to participate in a research protocol approved by the Committee on Clinical Investigation at Boston Children's Hospital.

## Author contributions

EJ, MT, JB, SG, PTS, FEV, CK, EM, and MD performed the experiments and analyzed the data. AS and SAT provided patient samples. EJ, AS, FWL, FB, and RSG designed and supervised the research. EJ, MT, and RSG wrote the manuscript.

## Acknowledgments

We thank Zach Herbert of the Molecular Biology Core Facilities at Dana-Farber Cancer Institute for library preparation and sample sequencing; and Joe Craft, Jason Weinstein, and Michael Carroll for their help and advice. This research was supported by NIH grants K08AI114968 (EJ) and R01AI114588 (RSG), and the Perkin Fund (RSG).

Address correspondence to: Erin Janssen or Raif S. Geha, Division of Immunology, Boston Children's Hospital, 1 Blackfan Circle, Karp Building 10th floor, Boston, Massachusetts 02115, USA. Phone: 617.919.2482; Email: erin.janssen@childrens.harvard.edu (E. Janssen); raif.geha@childrens.harvard.edu (R.S. Geha).

1. Song W, Craft J. T follicular helper cell heterogeneity: time, space, and function. *Immunol Rev*. 2019;288(1):85–96.
2. Trüb M, et al. Heterogeneity of phenotype and function reflects the multistage development of T follicular helper cells. *Front Immunol*. 2017;8:489.
3. Bossaller L, et al. ICOS deficiency is associated with a severe reduction of CXCR5+CD4 germinal center Th cells. *J Immunol*. 2006;177(7):4927–4932.
4. Choi YS, et al. ICOS receptor instructs T follicular helper cell versus effector cell differentiation via induction of the transcriptional repressor Bcl6. *Immunity*. 2011;34(6):932–946.
5. Xu H, et al. Follicular T-helper cell recruitment governed by bystander B cells and ICOS-driven motility. *Nature*. 2013;496(7446):523–527.
6. Schaerli P, Willimann K, Lang AB, Lipp M, Loetscher P, Moser B. CXC chemokine receptor 5 expression defines follicular homing T cells with B cell helper function. *J Exp Med*. 2000;192(11):1553–1562.
7. Schriever F, Korinth D, Salahi A, Lefterova P, Schmidt-Wolf IG, Behr SI. Human T lymphocytes bind to germinal centers of human tonsils via integrin alpha4/VCAM-1 and LFA-1/ICAM-1 and -2. *Eur J Immunol*. 1997;27(1):35–39.
8. Munoz MA, Biro M, Weninger W. T cell migration in intact lymph nodes in vivo. *Curr Opin Cell Biol*. 2014;30:17–24.

9. Zaretsky I, et al. ICAMs support B cell interactions with T follicular helper cells and promote clonal selection. *J Exp Med*. 2017;214(11):3435–3448.
10. Suzuki K, Grigorova I, Phan TG, Kelly LM, Cyster JG. Visualizing B cell capture of cognate antigen from follicular dendritic cells. *J Exp Med*. 2009;206(7):1485–1493.
11. Shulman Z, et al. Dynamic signaling by T follicular helper cells during germinal center B cell selection. *Science*. 2014;345(6200):1058–1062.
12. Kerfoot SM, et al. Germinal center B cell and T follicular helper cell development initiates in the interfollicular zone. *Immunity*. 2011;34(6):947–960.
13. Zotos D, et al. IL-21 regulates germinal center B cell differentiation and proliferation through a B cell-intrinsic mechanism. *J Exp Med*. 2010;207(2):365–378.
14. King IL, Mohrs M. IL-4-producing CD4+ T cells in reactive lymph nodes during helminth infection are T follicular helper cells. *J Exp Med*. 2009;206(5):1001–1007.
15. Shulman Z, et al. T follicular helper cell dynamics in germinal centers. *Science*. 2013;341(6146):673–677.
16. Victora GD, et al. Germinal center dynamics revealed by multiphoton microscopy with a photoactivatable fluorescent reporter. *Cell*. 2010;143(4):592–605.
17. Jabara HH, et al. DOCK8 functions as an adaptor that links TLR-MyD88 signaling to B cell activation. *Nat Immunol*. 2012;13(6):612–620.
18. Zhang Q, et al. Combined immunodeficiency associated with DOCK8 mutations. *N Engl J Med*. 2009;361(21):2046–2055.
19. Engelhardt KR, et al. Large deletions and point mutations involving the dedicator of cytokinesis 8 (DOCK8) in the autosomal-recessive form of hyper-IgE syndrome. *J Allergy Clin Immunol*. 2009;124(6):1289–302.e4.
20. Randall KL, et al. Dock8 mutations cripple B cell immunological synapses, germinal centers and long-lived antibody production. *Nat Immunol*. 2009;10(12):1283–1291.
21. Saunders SP, Ma EGM, Aranda CJ, Curotto de Lafaille MA. Non-classical B cell memory of allergic IgE responses. *Front Immunol*. 2019;10:715.
22. MacLennan IC. Germinal centers. *Annu Rev Immunol*. 1994;12:117–139.
23. Bannard O, Cyster JG. Germinal centers: programmed for affinity maturation and antibody diversification. *Curr Opin Immunol*. 2017;45:21–30.
24. Schwickert TA, et al. A dynamic T cell-limited checkpoint regulates affinity-dependent B cell entry into the germinal center. *J Exp Med*. 2011;208(6):1243–1252.
25. Kitano M, et al. Bcl6 protein expression shapes pre-germinal center B cell dynamics and follicular helper T cell heterogeneity. *Immunity*. 2011;34(6):961–972.
26. Dent AL, Shaffer AL, Yu X, Allman D, Staudt LM. Control of inflammation, cytokine expression, and germinal center formation by BCL-6. *Science*. 1997;276(5312):589–592.
27. De Silva NS, Klein U. Dynamics of B cells in germinal centres. *Nat Rev Immunol*. 2015;15(3):137–148.
28. Reimer D, et al. Early CCR6 expression on B cells modulates germinal centre kinetics and efficient antibody responses. *Immunol Cell Biol*. 2017;95(1):33–41.
29. Suan D, et al. CCR6 defines memory B cell precursors in mouse and human germinal centers, revealing light-zone location and predominant low antigen affinity. *Immunity*. 2017;47(6):1142–1153.e4.
30. Sage PT, Sharpe AH. T follicular regulatory cells in the regulation of B cell responses. *Trends Immunol*. 2015;36(7):410–418.
31. Breitfeld D, et al. Follicular B helper T cells express CXC chemokine receptor 5, localize to B cell follicles, and support immunoglobulin production. *J Exp Med*. 2000;192(11):1545–1552.
32. Ansel KM, McHeyzer-Williams LJ, Ngo VN, McHeyzer-Williams MG, Cyster JG. In vivo-activated CD4 T cells upregulate CXC chemokine receptor 5 and reprogram their response to lymphoid chemokines. *J Exp Med*. 1999;190(8):1123–1134.
33. Good-Jacobson KL, Szumilas CG, Chen L, Sharpe AH, Tomayko MM, Shlomchik MJ. PD-1 regulates germinal center B cell survival and the formation and affinity of long-lived plasma cells. *Nat Immunol*. 2010;11(6):535–542.
34. Weinstein JS, et al. TFH cells progressively differentiate to regulate the germinal center response. *Nat Immunol*. 2016;17(10):1197–1205.
35. Cannons JL, et al. Optimal germinal center responses require a multistage T cell:B cell adhesion process involving integrins, SLAM-associated protein, and CD84. *Immunity*. 2010;32(2):253–265.
36. Yusuf I, et al. Germinal center T follicular helper cell IL-4 production is dependent on signaling lymphocytic activation molecule receptor (CD150). *J Immunol*. 2010;185(1):190–202.
37. Xu J, et al. Mice deficient for the CD40 ligand. *Immunity*. 1994;1(5):423–431.
38. Kamperschroer C, Roberts DM, Zhang Y, Weng NP, Swain SL. SAP enables T cells to help B cells by a mechanism distinct from Th cell programming or CD40 ligand regulation. *J Immunol*. 2008;181(6):3994–4003.
39. Qi H, Cannons JL, Klauschen F, Schwartzberg PL, Germain RN. SAP-controlled T-B cell interactions underlie germinal centre formation. *Nature*. 2008;455(7214):764–769.
40. Lu KT, et al. Functional and epigenetic studies reveal multistep differentiation and plasticity of in vitro-generated and in vivo-derived follicular T helper cells. *Immunity*. 2011;35(4):622–632.
41. Dougall WC, Kurtulus S, Smyth MJ, Anderson AC. TIGIT and CD96: new checkpoint receptor targets for cancer immunotherapy. *Immunol Rev*. 2017;276(1):112–120.
42. Linden J, Cekic C. Regulation of lymphocyte function by adenosine. *Arterioscler Thromb Vasc Biol*. 2012;32(9):2097–2103.
43. Matozaki T, Murata Y, Okazawa H, Ohnishi H. Functions and molecular mechanisms of the CD47-SIRPalpha signalling pathway. *Trends Cell Biol*. 2009;19(2):72–80.
44. Günzel D, Fromm M. Claudins and other tight junction proteins. *Compr Physiol*. 2012;2(3):1819–1852.
45. Siegrist F, Ebeling M, Certa U. The small interferon-induced transmembrane genes and proteins. *J Interferon Cytokine Res*. 2011;31(1):183–197.
46. Liu KC, Cheney RE. Myosins in cell junctions. *Bioarchitecture*. 2012;2(5):158–170.
47. Halim D, et al. ACTG2 variants impair actin polymerization in sporadic megacystis microcolon intestinal hypoperistalsis syndrome.

*Hum Mol Genet*. 2016;25(3):571–583.
48. Braybrook C, et al. Identification and characterization of KLHL4, a novel human homologue of the Drosophila Kelch gene that maps within the X-linked cleft palate and Ankyloglossia (CPX) critical region. *Genomics*. 2001;72(2):128–136.
49. Islam SA, et al. Mouse CCL8, a CCR8 agonist, promotes atopic dermatitis by recruiting IL-5+ T(H)2 cells. *Nat Immunol*. 2011;12(2):167–177.
50. Rieck M, et al. Ceramide synthase 2 facilitates S1P-dependent egress of thymocytes into the circulation in mice. *Eur J Immunol*. 2017;47(4):677–684.
51. Reinhardt RL, Liang HE, Locksley RM. Cytokine-secreting follicular T cells shape the antibody repertoire. *Nat Immunol*. 2009;10(4):385–393.
52. Dustin ML, Springer TA. T-cell receptor cross-linking transiently stimulates adhesiveness through LFA-1. *Nature*. 1989;341(6243):619–624.
53. Wang Y, et al. LFA-1 affinity regulation is necessary for the activation and proliferation of naive T cells. *J Biol Chem*. 2009;284(19):12645–12653.
54. Gowthaman U, et al. Identification of a T follicular helper cell subset that drives anaphylactic IgE. *Science*. 2019;365(6456):eaaw6433.
55. Hoshino K, et al. Cutting edge: Toll-like receptor 4 (TLR4)-deficient mice are hyporesponsive to lipopolysaccharide: evidence for TLR4 as the Lps gene product. *J Immunol*. 1999;162(7):3749–3752.
56. Eisenbarth SC, Piggott DA, Huleatt JW, Visintin I, Herrick CA, Bottomly K. Lipopolysaccharide-enhanced, Toll-like receptor 4-dependent T helper cell type 2 responses to inhaled antigen. *J Exp Med*. 2002;196(12):1645–1651.
57. HogenEsch H, O'Hagan DT, Fox CB. Optimizing the utilization of aluminum adjuvants in vaccines: you might just get what you want. *NPJ Vaccines*. 2018;3:51.
58. Kool M, et al. Alum adjuvant boosts adaptive immunity by inducing uric acid and activating inflammatory dendritic cells. *J Exp Med*. 2008;205(4):869–882.
59. Shah HB, Devera TS, Rampuria P, Lang GA, Lang ML. Type II NKT cells facilitate alum-sensing and humoral immunity. *J Leukoc Biol*. 2012;92(4):883–893.
60. McSorley HJ, Blair NF, Robertson E, Maizels RM. Suppression of OVA-alum induced allergy by Heligmosomoides polygyrus products is MyD88-, TRIF-, regulatory T- and B cell-independent, but is associated with reduced innate lymphoid cell activation. *Exp Parasitol*. 2015;158:8–17.
61. Biram A, Davidzohn N, Shulman Z. T cell interactions with B cells during germinal center formation, a three-step model. *Immunol Rev*. 2019;288(1):37–48.
62. Janssen E, et al. DOCK8 enforces immunological tolerance by promoting IL-2 signaling and immune synapse formation in Tregs. *JCI Insight*. 2017;2(19):e94298.
63. Janssen E, et al. A DOCK8-WIP-WASp complex links T cell receptors to the actin cytoskeleton. *J Clin Invest*. 2016;126(10):3837–3851.
64. Randall KL, et al. DOCK8 deficiency impairs CD8 T cell survival and function in humans and mice. *J Exp Med*. 2011;208(11):2305–2320.
65. Ham H, et al. Dedicator of cytokinesis 8 interacts with talin and Wiskott-Aldrich syndrome protein to regulate NK cell cytotoxicity. *J Immunol*. 2013;190(7):3661–3669.
66. Lafouresse F, Cotta-de-Almeida V, Malet-Engra G, Galy A, Valitutti S, Dupré L. Wiskott-Aldrich syndrome protein controls antigen-presenting cell-driven CD4+ T-cell motility by regulating adhesion to intercellular adhesion molecule-1. *Immunology*. 2012;137(2):183–196.
67. Houmadi R, et al. The Wiskott-Aldrich syndrome protein contributes to the assembly of the LFA-1 nanocluster belt at the lytic synapse. *Cell Rep*. 2018;22(4):979–991.
68. Simonson WT, Franco SJ, Huttenlocher A. Talin1 regulates TCR-mediated LFA-1 function. *J Immunol*. 2006;177(11):7707–7714.
69. Meli AP, et al. The integrin LFA-1 controls T follicular helper cell generation and maintenance. *Immunity*. 2016;45(4):831–846.
70. Sage PT, Sharpe AH. In vitro assay to sensitively measure T(FR) suppressive capacity and T(FH) stimulation of B cell responses. *Methods Mol Biol*. 2015;1291:151–160.
71. Moriyama S, et al. Sphingosine-1-phosphate receptor 2 is critical for follicular helper T cell retention in germinal centers. *J Exp Med*. 2014;211(7):1297–1305.
72. Azcutia V, et al. CD47 plays a critical role in T-cell recruitment by regulation of LFA-1 and VLA-4 integrin adhesive functions. *Mol Biol Cell*. 2013;24(21):3358–3368.
73. Alcaide P, et al. Difference in Th1 and Th17 lymphocyte adhesion to endothelium. *J Immunol*. 2012;188(3):1421–1430.